

Supplementary information

Interaction of Nitrite with Ferric Protoglobin from *Methanosarcina acetivorans* - An Interesting Model for Spectroscopic Studies of the Haem-Ligand Interaction

Roberta Sgammato,^{#a} Niels Van Brempst,^{#b,c} Roy Aerts,^a Sabine Van Doorslaer,^b Sylvia Dewilde,^{‡c} Wouter Herrebout,^a and Christian Johannessen^{*a}

a. Laboratory of Molecular Spectroscopy, Department of Chemistry, University of Antwerp, Groenenborgerlaan 171, B-2020 Antwerp, Belgium.
E-mail: christian.johannessen@uantwerpen.be

b. Laboratory of Biophysics and Biomedical Physics, Department of Chemistry, University of Antwerp, Universiteitsplein 1, B-2610 Wilrijk, Belgium.

c. Laboratory of Protein Sciences, Proteomics and Epigenetic Signaling, Department of Biomedical Sciences, University of Antwerp, Universiteitsplein 1, B-2610 Wilrijk, Belgium.

‡ Prof. Dr. Sylvia Dewilde passed away during the preparation of the manuscript

authors contributed equally

Sequence of C-terminal His₆-tagged *MaPgb*

MSVEKIPGYT YGETENRAPF NLEDLKLLKE AVMFTAEDDEE
YIQKAGEVLED QVEEILDW YGFVGSHPHL LYYFTSPDGT
PNEKYLA AVR KRFSRWILDT CNRSYDQAWL DYQYEIGLRH
HRTKKNQTDN VESVPNIGYRY LVAFIYPIT ATMKPFLARK GHTPEEVEKM
YQAWFKATTL QVALWSYPYV YGDFLEHHH HHH

Supplementary Figure S1: Absorbance and ECD spectra of ferric *MaPgb* and myoglobin at pH 7.5.

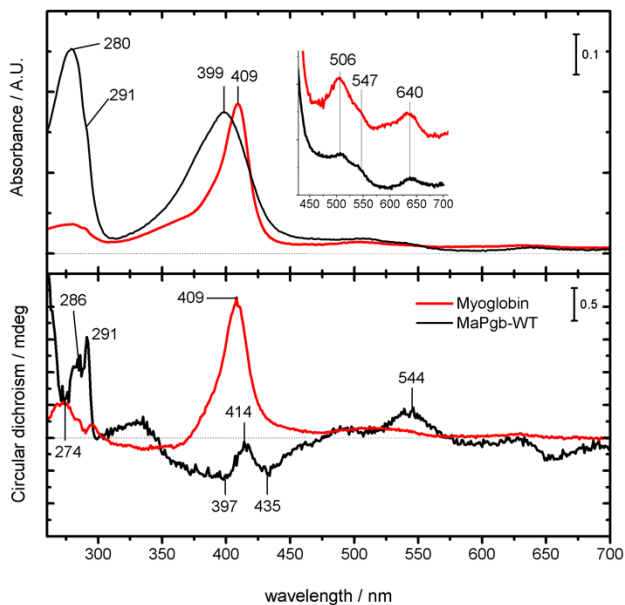


Figure S1 As-purified ferric *MaPgb* (black) in comparison with ferric myoglobin (aquomet form, red), both measured Trizma® hydrochloride buffer at pH 7.5. Absorption (top) and ECD (bottom) spectra were recorded in the spectral region 260-700 nm.

Supplementary Figure S2: secondary structure of ferric *MaPgb*

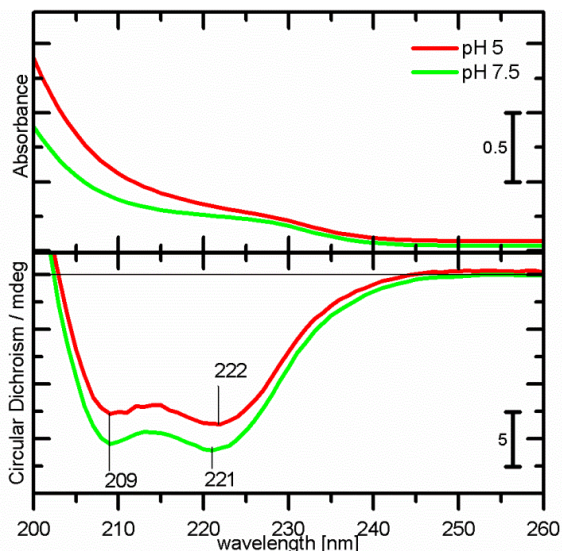


Figure S2 Ferric *MaPgb* (0.056 mM of haem content) at pH 7.5 (green) in comparison with ferric *MaPgb* at pH 5 (red), measured in Trizma® hydrochloride buffer and acetate buffer, respectively. Absorption (top) and ECD (bottom) spectra were recorded in the spectral region 200-260 nm.

Supplementary Table S1: Spectroscopic characterization of *MaPgb* after addition of nitrite

	Abs-Spectroscopy / nm				Assign	rRaman / cm^{-1}			
	Soret	Q_{β} (nm)	Q_{α}	CT		ν_4 (cm^{-1})	ν_3	ν_2	ν_{10}
MaPgb Fe(III)	399	506	547	638	5C/HS	1376	1460	1573	1631
1:50	405		556						1631
1:100	421	538	570			1376	1460/1506	1578	1631
1:200	425	538	570		6C/LS	1376	1460/1506	1578	1631
1:300	425	538	570		6C/LS				1631
1:400	425	538	570		6C/LS	1376	1460/1506	1580	1631

Table S1: Main Abs and rRaman bands of Fe(III) *MaPgb* and Fe(III) *MaPgb* in complex with nitrite

Supplementary Figure S3: Low frequency rRaman spectrum of MaPgb upon nitrite treatment

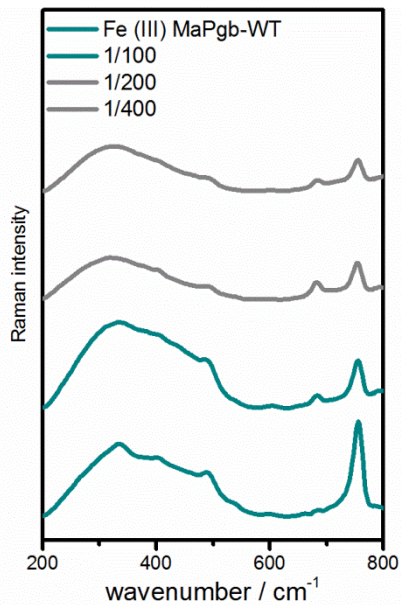


Figure S3 rRaman spectra of 0.057 mM *MaPgb* and its complexes with nitrite in sodium acetate buffer at pH 5 in the spectral range 200–800 cm⁻¹. *MaPgb* (0.056 mM of haem content) was incubated with 50, 100, 200 and 400 molar ratio excess nitrite, respectively.

Supplementary Table S2: rRaman characterization of ferric *MaPgb*

This work (5c/QS)			Reference (Mb)	
Mode	Wavenumber /cm ⁻¹	Assignment	Authors	Wavenumber /cm ⁻¹
v10	1631	5C/HS C=C vinyl stretch	A1	
v2	1573	5C/HS	A1	1573
v11/v2	1552	6C/HS	A1	1556
v3	1460	5C/HS(FeII)	A1	1470
	1437			
v29	1405		A2	1403
v4	1376	5C/HS	A1	1368-1374
v41	1344		A2	1341
v21	1307	$\delta(\text{C}_a\text{H}=\text{)}_{4 \text{ or } 2}$	A2	1301-1316
	1227			
v30	1165		A2	1169
v14	1127		A2	1121
	1081			
v45	999	(C _{β} -vinyl stretch)	A2	989
	923	$\gamma(\text{C}_b\text{H}_2)_s$	A2	919
	844			
v16	755		A3	751
	686			
v48	599		A3	605
γ 21	540			547
	490			
	403	$\delta(\text{C}_\beta\text{C}_a\text{C}_b)_4$	A2	405
γ 6	335		A2	337
	233			

Table S2: Position of main rRaman marker bands of ferric *MaPgb* and their assignments.

References: A1 = reference [32] in main text; A2 = S. Hu, K. M. Smith, T. G. Spiro, J. Am. Chem. Soc., 1996, 118, 12638; A3 = reference [22] in main text.

Supplementary Figure S4. Low-temperature EPR spectra of ferric *MaPgb* with and without nitrite

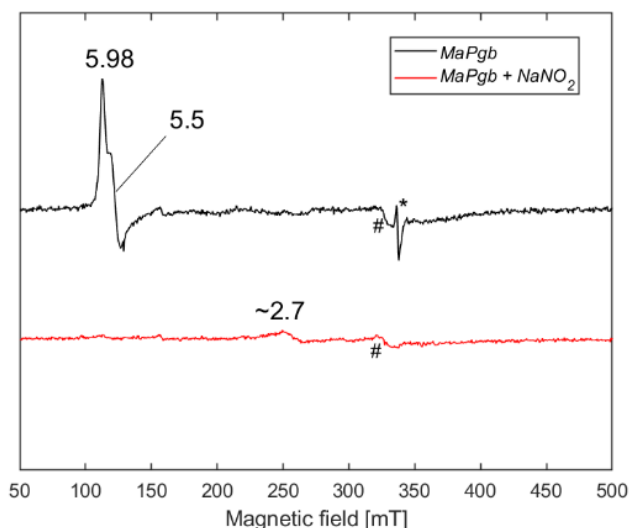


Figure S4 Low-temperature (10 K) CW EPR spectra of ferric *MaPgb* at pH 5 (sodium acetate buffer) without (black) and with (red) sodium nitrite (1:400 *MaPgb*:*NaNO*₂). 25% glycerol (v/v) was added as cryoprotectant. # is due to a background signal (*Cu*^{II}). Asterisk shows the presence of radical contaminant.

The EPR spectrum of ferric *MaPgb* can be ascribed by a rhombic effective *g* tensor, indicative of an admixture of the *S*=5/2 state with an *S*=3/2 state (formation of a QS state) [ref: M. M. Maltempo, *J. Chem. Phys.*, 61, 2540 (1974)]. Since glycerol was added as a cryoprotectant to the sample, it is unclear whether the here observed signal is due to a 5*c*/QS or a 6*c*/QS species. In any case, the EPR confirms the occurrence of QS states in ferric *MaPgb*.

Addition of sodium nitrite to ferric *MaPgb* leads to a disappearance of the EPR signal of the ferric component in line with the formation of an EPR-silent NO-ligated ferric haem complex. No signal of ferrous nitrosylated *MaPgb* is observed, confirming that NO binding to the ferric form is not succeeded by a further reductive nitrosylation step as is observed at pH 7 and higher (reference [14] in main text).

Supplementary Figure S5: Protein stability in the presence of nitrite.

To rule out the possible denaturation of *MaPgb* in presence of high concentration of nitrite at pH5, far-UV ECD spectra were recorded (Fig. S5). ECD spectra of *MaPgb* (0.0056 mM in haem concentration) incubated with 0.28, 0.56, 1.12, 1.68 and 2.24 mM NaNO_2 in sodium acetate buffer (pH 5), were measured in the range 260–195 nm.

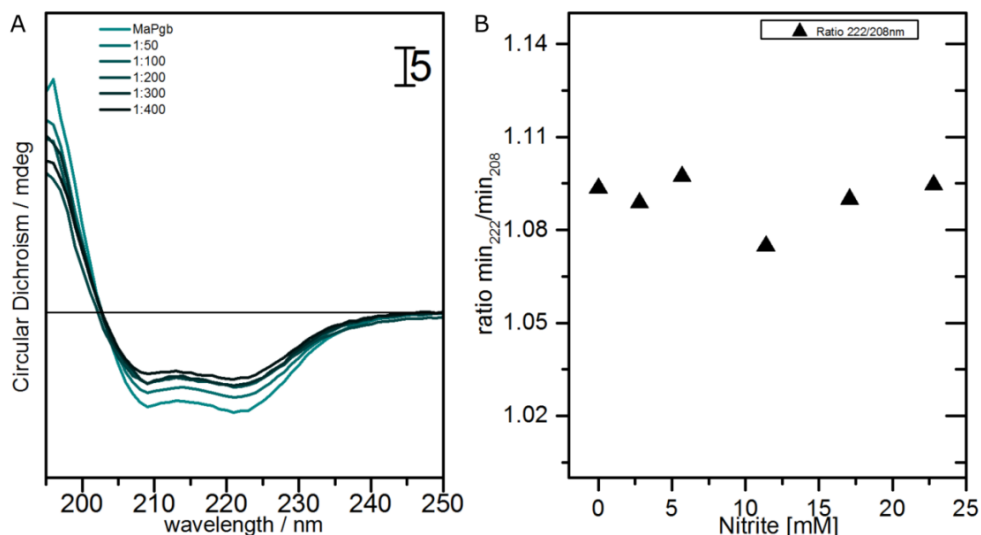


Figure S5: Panel A: ECD spectra of *MaPgb* (0.056 mM in haem concentration) in complex with sodium nitrite in sodium acetate buffer at pH 5 in the spectral range 195-250 nm; Variations in the 222/208 nm ratio as function of the concentration of NaNO_2 used for the sample treatment at pH 5 (black triangle) are reported in Panel B.

In the far-UV region of the ECD spectrum (Fig. S5, Panel A) the presence of the two negative minima at 208 nm and 222 nm clearly indicated the alpha-helix secondary structure of *MaPgb*. Since the variation in the ratio between the ellipticity measured at 222 and 208 nm is indicative of the protein structural changes, it was plotted as function of the nitrite concentration incubated with *MaPgb* for the treatments at the pH values of 5. Minor variations were found in the 222/208 nm ratio when the concentration of the ligand was increased, as well as an overall decrease of the ECD intensity, indicating the unfolding of a minor fraction of the protein in presence of nitrite at mildly acidic pH values occurred. Nevertheless, the treatment of the globin with increasing amount of nitrite in mildly acidic conditions did not affect the spectra drastically.

Moreover, the ellipticity detected in the range 300-600 nm intrinsically proved that the haem chromophore was correctly located into the protein matrix. A total loss of the haem group as consequence of the protein degradation, would imply the disappearance of all optical activity of the protein in that specific spectral range (Fig. S14). Therefore, we could conclude that the secondary structure composition was retained during the nitrite treatment.

Supplementary Figure S6 – pH variation

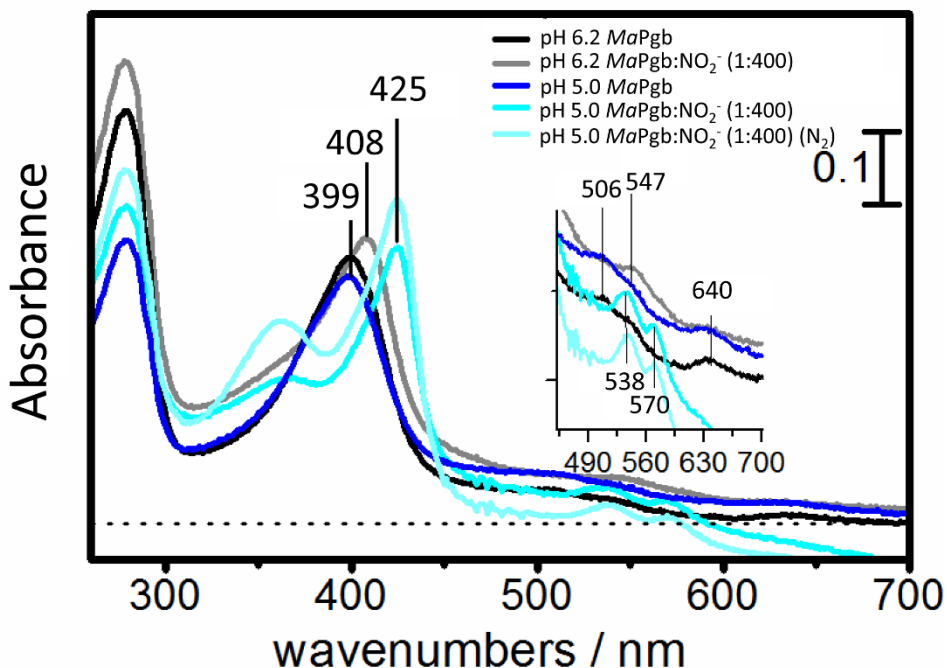


Figure S6: Absorption spectra of ferric *MaPgb* (0.057 mM in haem content) at pH 5.0 (dark blue) and pH 6.2 (black). Effect of addition of a 400-fold excess of sodium nitrite to ferric *MaPgb* (0.057 mM in haem content) at pH 6.2 (grey) and pH 5 (cyan). The effect of the reaction in N₂ and with addition of air was also tested.

While the clear signature of a full conversion of ferric *MaPgb* to its Fe(III)-NO form is observed at pH 5 upon addition of a 400x excess of sodium nitrite, only the onset of the transformation can be seen at pH 6.2. At pH 7.5, no nitrosylated ferric *MaPgb* was observed under the same conditions (not shown). This indicates that pH plays a role in the formation of Fe(III)-NO form. The spontaneous decomposition of nitrite with formation of NO is known to increase significantly at lower pH (NO-formation rate in 22.8 mM NaNO₂ at pH 5 is $4.48 \cdot 10^{-7}$ M/s and at pH 6.2 is $2.88 \cdot 10^{-8}$ M/s) [Reference: A. Samouilov, P Kuppusamy, J. L. Zweier, *Arch. Biochem. Biophys.* 1998, 357 1].

Supplementary Table S3. Bi-exponential fit to the time traces in Figure 6D.

	k_f / s^{-1}	k_s / s^{-1}	C(1)	C(2)	C(3)
1:400 <i>MaPgb</i> :NO ₂ ⁻	17.35 10 ⁻³ (±1.5 10 ⁻³)	0.92 10 ⁻³ (±0.04 10 ⁻³)	97.6 (±0.5)	58.4 (±1.9)	39.1 (±1.4)
1:100 <i>MaPgb</i> :NO ₂ ⁻	3.39 10 ⁻³ (±0.4 10 ⁻³)	0.21 10 ⁻³ (±0.01 10 ⁻³)	61.2 (±0.5)	20.2 (±0.9)	38.8 (±0.5)

Supplementary Figures S7-S13: TMA-PTIO spin-trapping experiments

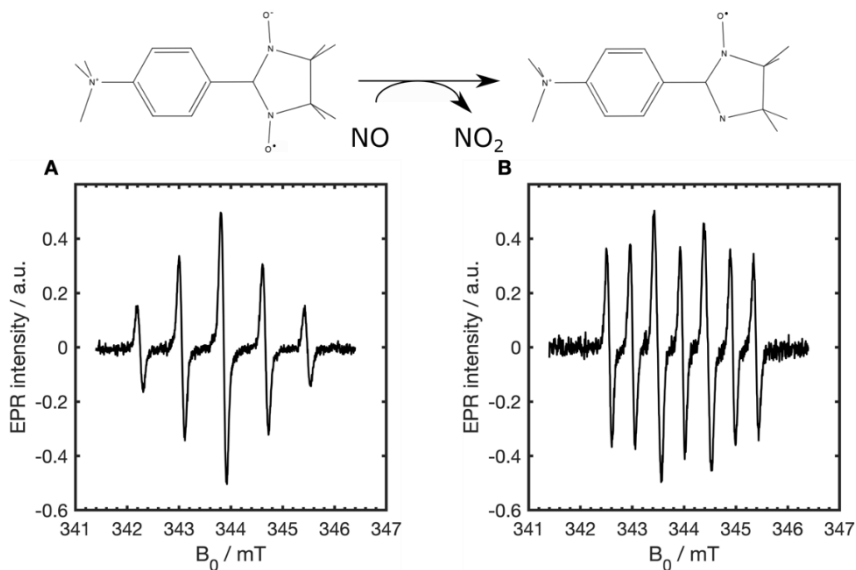
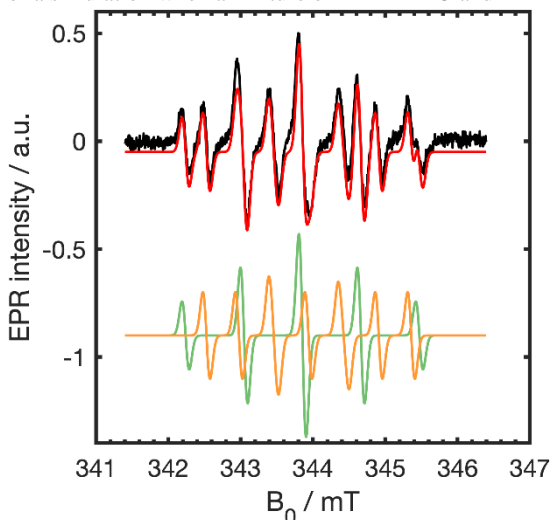


Figure S7: Reaction mechanism of TMA-PTIO (A) to TMA-PTI (B) conversion in the presence of NO. The corresponding room temperature X-band CW-EPR spectra are given underneath the chemical structures of the radicals.

Figure S8: Illustration of a simulation when a mixture of TMA-PTIO and TMA-PTI is present. The X-



band CW-EPR spectrum at room temperature (black) is simulated (red) and consists of the sum of contributions of TMA-PTIO (lime green) and TMA-PTI (gold). The spectrum of pure TMA-PTIO consists of 5 lines which can be simulated using a system with two equivalent ^{14}N nuclei, with the isotropic hyperfine value $A = 22.69$ MHz and a g -factor of 2.0082. The spectrum of TMA-PTI consists of 7 lines and can be simulated using two inequivalent ^{14}N nuclei with inequivalent hyperfine values 12.63 and 27.17 MHz and a g -factor of 2.0077.

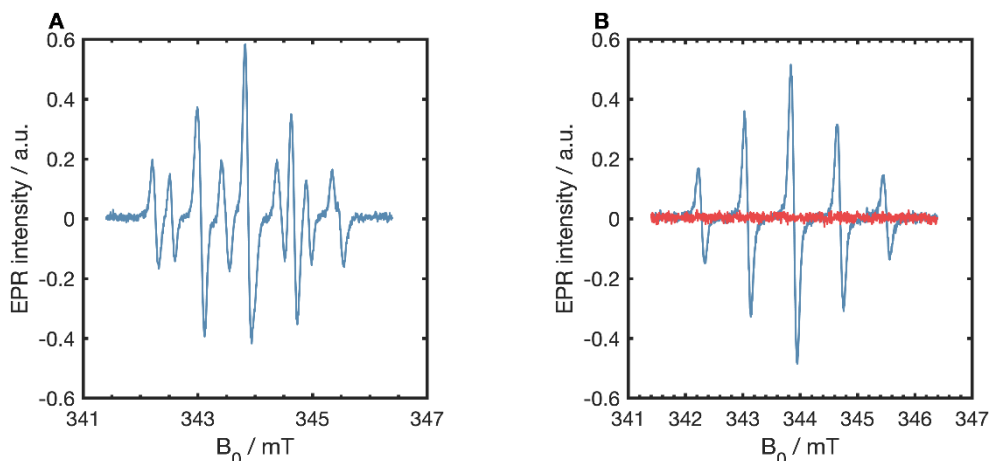


Figure S9: Panel A shows the room temperature X-band CW-EPR spectrum of 25 μM TMA-PTIO when an excess of NONOate is added at pH 7.5. The appearance of the EPR signal of TMA-PTI shows the effectiveness of TMA-PTIO as an NO spin trap. Panel B shows that 10 μM *MaPgb* without addition of NaNO_2 (2.5x molar excess, blue), does not lead to TMA-PTI formation, and that *MaPgb* itself without TMA-PTIO (red) does not contribute to the total signal intensity at room temperature.

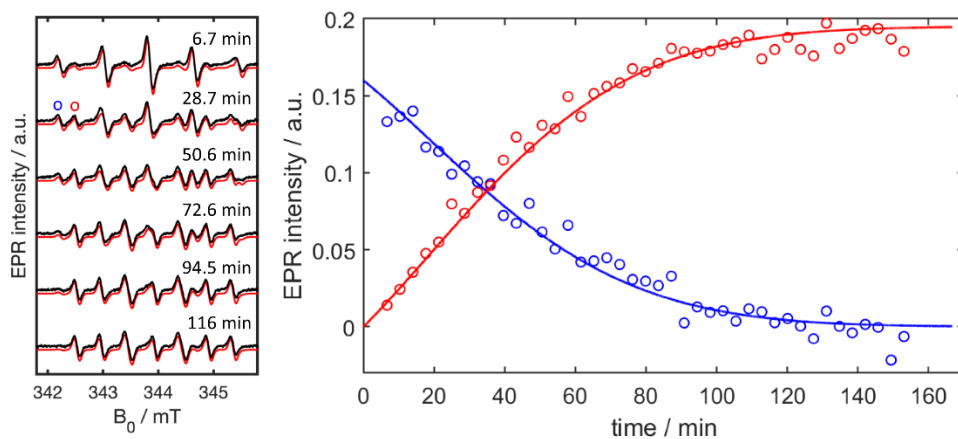


Figure S10: Left: the room temperature X-band CW-EPR spectra (black) and corresponding simulations (red) of 25 μM TMA-PTIO collected over time after addition of 4 mM nitrite. The experiments were performed in a sodium acetate buffer at pH 5. All spectra were collected with a microwave power $P=1.5\text{mW}$ and a modulation amplitude of 0.1 mT. Each simulation consists of a linear combination of the spectra of pure TMA-PTIO and TMA-PTI, respectively. Over time, TMA-PTIO is converted to TMA-PTI. Right: time dependence of the experimental signal intensity of TMA-PTIO (represented by the peak maximum indicated by 'o' in the left spectrum) and TMA-PTI (represented by the peak maximum 'o' in the left spectrum). The solid lines are simulations considering the model described below.

Figure S10 (right) shows the time-dependent conversion of TMA-PTIO to TMA-PTI as it traps nitric oxide that is formed spontaneously in a 4mM sodium nitrite solution at pH 5. The time dependence can be simulated using a simple model in which the

concentration of NO is predicted using the NO formation rate described in [Reference: A. Samouilov, P Kuppusamy, J. L. Zweier, *Arch. Biochem. Biophys.* 1998, 357, 1-7]

$$\frac{d[NO]}{dt} = \frac{K_1[NO_2^-][HNO_2]}{[NO_2^-] + K_\beta}, \quad (1)$$

with

$$[HNO_2] \cong \frac{[H^+][NO_2^-]_0}{[H^+] + K_\alpha}; \quad [NO_2^-] \cong \frac{K_\alpha[NO_2^-]_0}{[H^+] + K_\alpha}.$$

The trapping of NO is then described by the simple equation

$$\frac{d[TMA - PTIO]}{dt} = -k_1[TMA - PTIO][NO].$$

The build-up of TMA-PTI evidently follows the decay of TMA-PTIO

$$\frac{d[TMA - PTI]}{dt} = k_1[TMA - PTIO][NO].$$

In order to fit the decay curve in Figure 10, the initial concentration of NO needed to be taken different from zero, in line with the fact that the nitrite was added from a concentrated stock solution in which nitrite disproportionation will have been initiated ($[NO]_0 = 100\text{-}300 \mu\text{M}$ depending on batch). The curves in Figure S10 are fitted assuming $[NO]_0 = 150 (\pm 50) \mu\text{M}$ and $k_l = 1.3 (\pm 0.2) \text{M}^{-1}\text{s}^{-1}$.

The decay curve (blue circles) can also be fitted satisfactorily with an apparent first-order dependence, with a rate constant $2.4 (\pm 0.5) 10^{-4} \text{s}^{-1}$. Although this rate constant has no physical meaning it can serve to compare with the apparent first-order reaction constants k_f and k_s , observed for the formation of *MaPgb*-NO (Table S3).

The time-dependence of the EPR spectra of TMA-PTIO and TMA-PTI in the presence of nitrite and ferric *MaPgb* (Figure 7B) or ferric Mb (Figure S11) can be satisfactorily simulated using the same model as introduced above for the protein-free case. The only exception is that the build-up of TMA-PTI is now followed by a decay phase in which TMA-PTI is degenerated towards other products. This is introduced in the model assuming

$$\frac{d[TMA - PTI]}{dt} = k_1[TMA - PTIO][NO] - k_2[TMA - PTI].$$

The curves in Figure S11 and Figure 7B can both be satisfactorily fitted assuming $[\text{NO}]_0 = 300 (\pm 50) \mu\text{M}$, $k_1 = 1.3 (\pm 0.2) \text{ M}^{-1}\text{s}^{-1}$ and $k_2 = 6.5 \cdot 10^{-5} (\pm 1.0 \cdot 10^{-5}) \text{ s}^{-1}$.

The similarity in the decay parameters indicates that the presence of *MaPgb* does not alter significantly the ability of TMA-TPIO to trap NO and hence provides no clear proof of a specific nitrite dismutase activity.

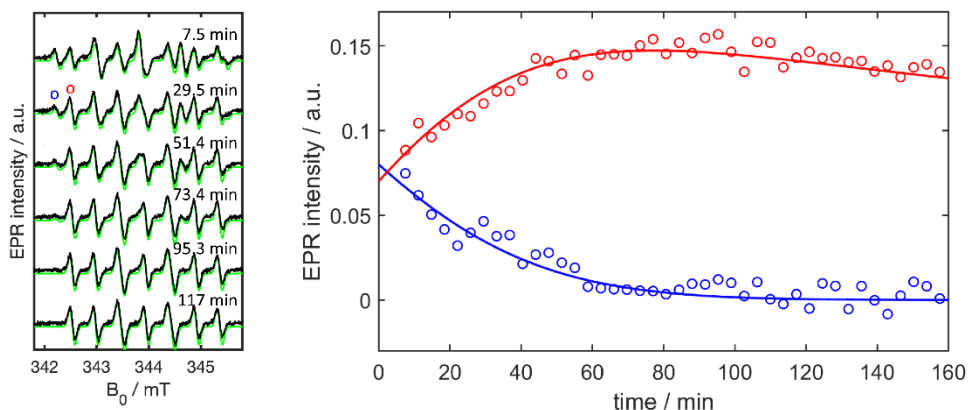


Figure S11: Left: the room temperature X-band CW-EPR spectra (black) and corresponding simulations (green) of $25 \mu\text{M}$ TMA-PTIO in the presence of $10 \mu\text{M}$ ferric Mb collected over time after addition of 4 mM nitrite. The experiments were performed in a sodium acetate buffer at pH 5. All spectra were collected with a microwave power $P=1.5\text{mW}$ and a modulation amplitude of 0.1 mT . Each simulation consists of linear combination of the spectra of pure TMA-PTIO and TMA-PTI, respectively. Over time, TMA-PTIO is converted to TMA-PTI. Right: time dependence of the experimental signal intensity of TMA-PTIO (represented by the peak maximum indicated by ‘o’ in the left spectrum) and TMA-PTI (represented by the peak maximum ‘o’ in the left spectrum). The solid lines are simulations considering the model described below.

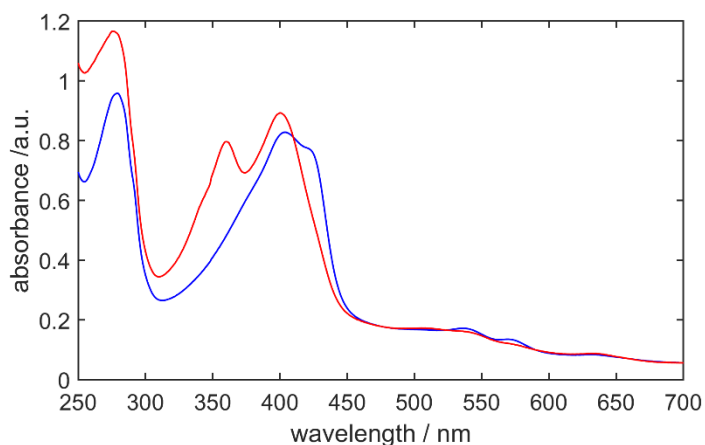


Figure S12: Comparison between the UV/Vis absorption spectrum of ferric *MaPgb* at pH 5.0 (10 μ M in haem content) overnight incubated with 1 mM sodium nitrite (blue) and the spectrum measured immediately after addition of 25 μ M TMA-PTIO to the mixture (red).

While an incubation of *MaPgb* with nitrite (1:100 ratio) only leads to formation of a limited fraction of *MaPgbNO*, this protein was rapidly depleted from NO by addition of TMA-PTIO (Fig. S12). This shows the ability of *MaPgb* to exchange NO with TMA-PTIO.

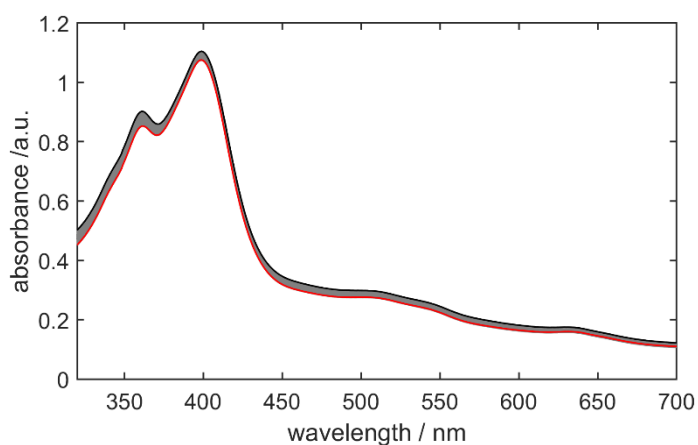


Figure S13: Optical absorption spectra collected over time of *MaPgb* (10 μ M haem concentration) reacted with 1 mM sodium nitrite in a sodium acetate buffer at pH 5 in presence of 25 μ M TMA-PTIO at 20°C. The black trace shows the absorption spectrum before addition of nitrite, the red trace shows the absorption spectra at the end of the time trace (after 245 minutes).

Supplementary Figure S14: Visible absorption and ECD spectrum of Hemin

Hemin was measured in pure water in free form and after incubation with nitrite. In the absorption spectrum a broad positive band with maximum at 392 nm was observed. As expected, no ECD signal was observed, showing that the molecule in solution does not exhibit optical activity. Nitrite was added to the sample in final concentration of 22.4mM, and new absorption ECD spectra were recorded. A new absorption band at 356 nm was observed corresponding to nitrite, and again no ellipticity was observed.

The experiment shows that the ECD signals of ferric *MaPgb* treated with nitrite (Fig. 3) can only be ascribed to the haem-ligand complex correctly incorporated in the protein matrix.

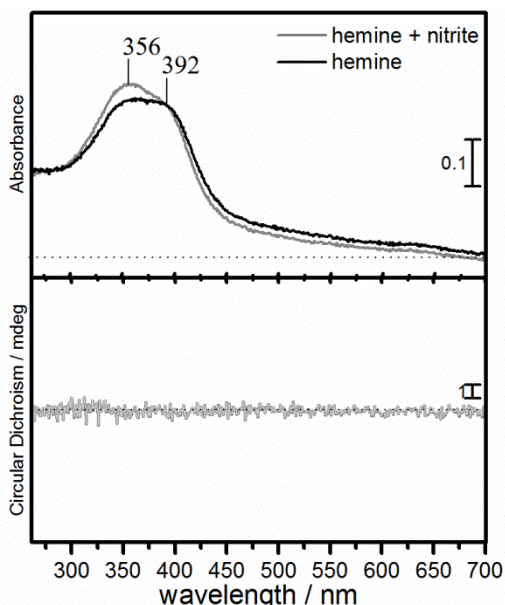


Figure S14: Absorption (top) and ECD (bottom) spectra of hemin in water (black) and complex with 22 μ M sodium nitrite (gray) in the spectral range 260-700 nm.

Supplementary Figure S15: Haem pocket visualizations of *MaPgb* and Mb.

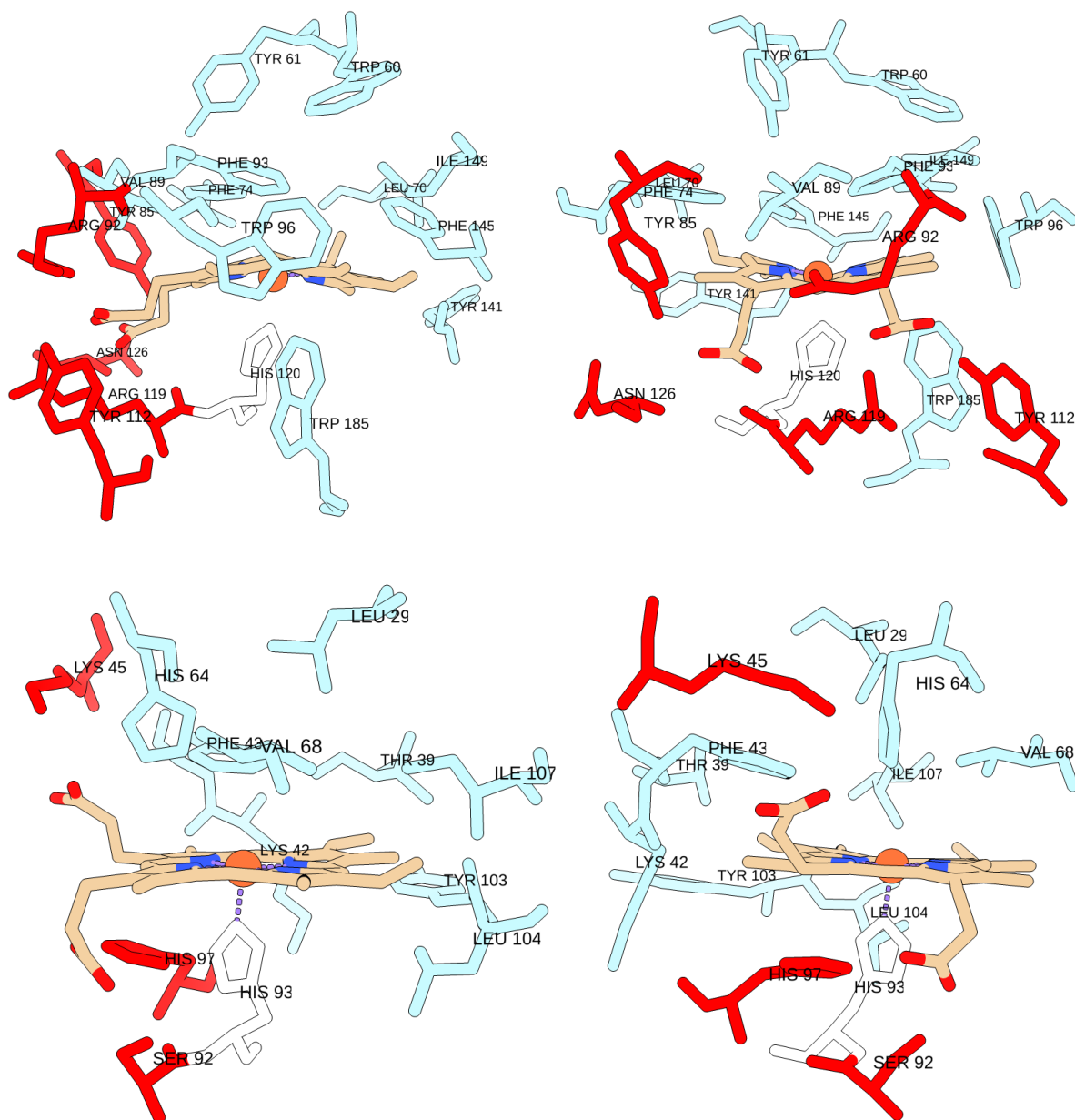


Figure S15 Visualizations of the haem group and pocket of *MaPgb* (PDB entry 2VEE; top figures) and Mb (PDB entry 1AZI; bottom figures). The side chains of the residues that interact with the propionate haem side chains are depicted in red, the ones constituting the haem pocket are light blue, and the proximal histidine coordinating the central iron is white.

Supplementary Figure S16 – Simulation of dependence on nitrite concentration

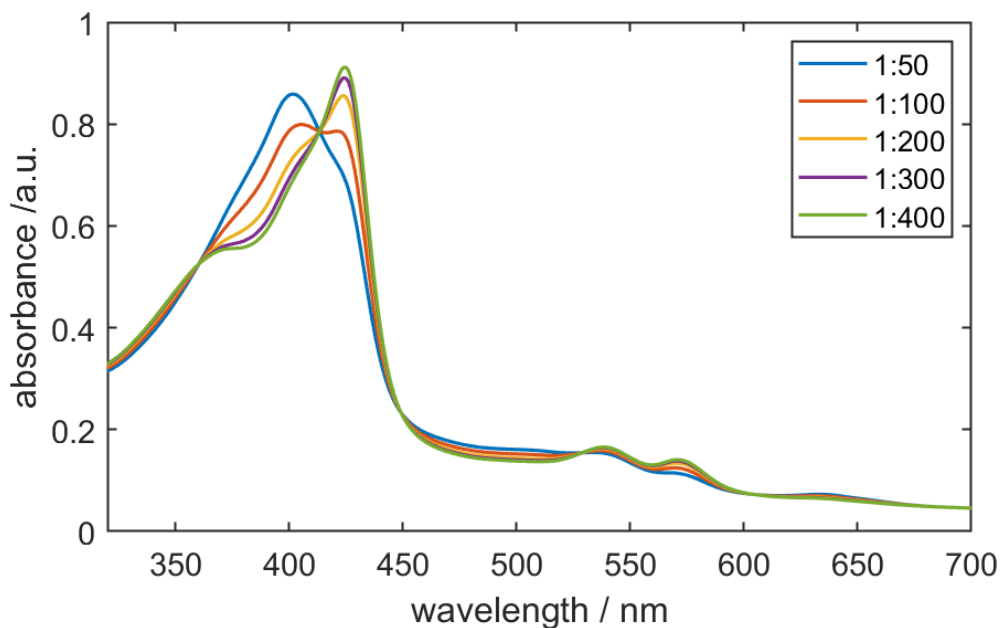
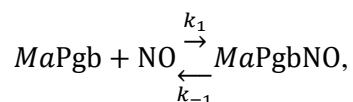


Figure S16: Reconstructed UV/Vis-absorption spectra using weighted percentages of the absorption spectra of ferric *MaPgb* and ferric *MaPgbNO* as described below.

Within the range of nitrite concentrations used in the experiments shown in Figure 3, the concentration of NO formed due to spontaneous disproportionation scales approximately with the nitrite concentration for a fixed pH [Reference: A. Samouilov, P Kuppasamy, J. L. Zweier, *Arch. Biochem. Biophys.* 1998, 357, 1-7].

Hence, a change of the nitrite concentration by a factor N will also change the NO concentration present after a time t by a factor N . If the observed ferric *MaPgbNO* is due to simple trapping of NO *via*



the relative ratio of $[\text{MaPgbNO}]/[\text{MaPgb}]$ can be easily written as

$$\frac{[\text{MaPgbNO}]}{[\text{MaPgb}]} = K_{eq}[\text{NO}] = \frac{k_1}{k_{-1}}[\text{NO}] = \frac{x}{10 - x},$$

with x the concentration of $MaPgbNO$ in μM . Using the UV/Vis-spectra of ferric $MaPgb$ and $MaPgbNO$, the ratio $\frac{[MaPgbNO]}{[MaPgb]}$ can be determined from the UV-Vis spectrum of $MaPgb$ incubated with a 100-fold excess of nitrite. When assuming that the NO concentration changes with the same factor as the nitrite concentrations, the spectra of the 50-fold, 200-fold, 300-fold and 400-fold excess cases can then be predicted using the relative contributions of $MaPgb$ and $MaPgbNO$ determined using the above equation. Figure S16 shows the absorption spectra obtained in this way. These absorption spectra match very well with the ones observed in Figure 3 (main text), showing that the equilibrium state can be described based on the ligation of only one ligand (presumably NO). This argues against a binding of two nitrite molecules as would be expected for nitrite dismutase.

Open data

Raw data can be found on the Open Science Framework <https://osf.io/hpfzt/> (data opened to public upon publication of the manuscript).